Hematology and Thromboembolic Diseases: Open Access

Yang et al., J Hematol Thrombo Dis 2014, 2:3
http://dx.doi.org/10.4172/2329-8790.1000137

Research Article Open Access

Photothermal Targeting Therapy of A20 Mouse Lymphoma Model using Anti-CD138 Antibody-conjugated Gold Nanospheres

Huimin Meng[1*], Yunhui Zong[1*], Jianfei Qian[2], Yu Jing[3], Jinle Tang[1], Jianxuan Zou[1], Gangli An[1], Hui Song[2,4,5], Xingding Zhang[2,4,5], and Lin Yang[1]

[1]*The Cyrus Tang Hematology Center, Soochow University, Suzhou, Jiangsu, PR China*

[2]*Xi'an Jiaotong University Suzhou Academy, Suzhou, Jiangsu, PR China*

[3]*Department of Hematology, the General Hospital of the PLA, Beijing, PR China*

[4]*Suzhou Cancer Immunotherapy and Diagnosis Engineering Center, Suzhou, Jiangsu, PR China*

[5]*PersonGen Biomedicine (Suzhou) Co., Ltd., Suzhou, Jiangsu, PR China*

[*]**Corresponding author:** Lin Yang, The Cyrus Tang Hematology Center, Soochow University, 199 Ren'ai Road, SIP, Suzhou, Jiangsu, PR China, Tel: +86 -512- 6588 0877; Fax: +86 -512-6588 1544; E-mail: yanglin@suda.edu.cn

Rec date: Mar 3, 2014, **Acc date:** Apr 12, 2014, **Pub date:** Apr 18, 2014

Abstract

The aim of this study was to investigate the therapeutic effects of photothermal targeting of hollow gold nanospheres on lymphoma. Hollow gold nanospheres were modified by PEG (polyethylene glycol) and conjugated to anti-CD138 antibody. The conjugates were then injected into the A20 mouse lymphoma model followed by near-infrared laser radiation (NIR). By examining the level of immunoglobulin G2a secreted by A20 cells and measuring the weight of specimen biopsy, tumorgenesis was determined. Finally, the possibility of lymphoma-targeted photothermal therapy was evaluated. Anti-CD138 antibody-conjugated hollow gold nanospheres (HAuNs-CD138) were prepared and the A20 mouse lymphoma model was established. After NIR treatment, A20 lymphoma growth was significantly suppressed. HAuNs-CD138 treatment represents a potential therapeutic strategy for CD138+ lymphoma.

Keywords: Lymphoma; A20 lymphoma cells; Gold nanosphere; Photothermal therapy; Cancer-targeting therapy

Introduction

Traditionally, treatments for lymphoma include chemotherapy, radiotherapy, and immunotherapy, among which chemotherapy is the principal treatment for blood tumors represented by lymphoma, but the emergence of drug resistance to chemotherapy makes it an urgent task to seek new treatments. Recently, photothermal therapy based on nanoparticles has become an attractive novel cancer treatment strategy [1-7]. One of the most striking innovations is the combination of noble metal nanoparticles and photics. Noble metal nanoparticles show strong extinction and strong scattering effects by near-infrared laser radiation (NIR, near-infrared region, wavelength 700–850 nm), due to surface plasmon resonance (SPR) [8-11]. It is remarkable that the wavelength range shows minimum absorbance for biological tissue and good penetration. These properties make gold nanoparticles a vital option for cancer treatment.

In recent years, second-generation hollow gold nanospheres (HAuNS) were developed [12]. This nanostructure combines small size (outer diameter is only 30 to 60 nm), spherical shape, hollow interior, and strong and tunable absorption band (520–950 nm), constituting a highly unique nanostructure [12,13]. When this type of nanoparticle is coated by polyethylene glycol (PEG), HAuNS under 100 nm in diameter show significantly prolonged half-life in the circulatory system [14,15]. By enhancing permeability and retention [16], HAuNS with the ability of long cycle have a greater probability of penetrating tumor vascular structures, reaching tumor tissue eventually. Because passive diffusion of nanoparticles to tumor tissue is mainly affected by the perforation diameter of the tumor vessel wall, obviously, smaller HAuNS have an advantage over the bigger nanostructure formed by a silica core in terms of penetrating the tumor vessel wall. Indeed, it has been confirmed that the perforation diameter of tumor vessel wall is only about 7 to 100 nm in gliomas and ovarian cancer [17,18].

Here, we describe a new type of active targeting photothermal therapeutic agent, HAuNS-CD138, applied in lymphoma mouse model treatment. CD138 (also known as syndecan-1), a 220 kDheparan sulfate proteoglycan, acts as an adhesion molecule and is widely expressed on the cell surface of multiple myeloma, leukemia, and lymphoma [19], which makes CD138 a potential therapeutic target for lymphoma. The A20 lymphoma mouse model established here was intraperitoneally injected with HAuNs-CD138, and after NIR treatment, A20 lymphoma growth was significantly suppressed. In conclusion, we have successfully prepared an active targeting photothermal therapeutic agent of HAuNs-CD138 nanoparticles and results in an animal model have suggested that HAuNs-CD138 nanoparticles are a potential therapeutic approach in CD138+ malignancies.

Materials and Methods

Main materials

The A20 mouse lymphoma cell line was provided by the Department of Myeloma and Lymphoma, MD Anderson Cancer Center (USA). A20 cells were maintained at 37°C in a humidified atmosphere containing 5% CO_2 in RPMI (Roswell Park Memorial Institute) 1640 medium and 10% fetal bovine serum (Life

Technologies, Inc., Grand Island, NY, USA). Female 6- to 8-week-old BALB/c mice were purchased from the Animal Facility, Soochow University (China), and anti-CD138 antibody was purchased from BD Biosciences (USA). Trifluoroacetic acid, triethylsilane and piperidine were purchased from Chem-Impex International (USA). Methoxy-PEG-SH (MW 5000) was purchased from Nektar (USA). NH2-PEG-COOH.HCl (MW 5000) was purchased from JenKem Technology (USA). Cobalt chloride hexahydrate, sodium borohydride, chloroauric acid trihydrate, hydroxylamine, and dialysis bag were purchased from Fisher Scientific (USA). PD-10 Spin Column was purchased from Amersham-Pharmacia Biotech (China).

Synthesis of HAuNS-CD138

PEG-modified HAuNS were provided by Pro. Chun Li (MD Anderson Cancer Center, USA). The antibodies were first conjugated to one end of the PEG chain to prepare CD138-PEG-SH [13], and then HAuNS (8.5×1012 particles/mL) were added to an argon-purged aqueous solution containing CD138-PEG-SH (50 μg/mL) and PEG-SH (500 μg/mL). The reaction was allowed to proceed overnight at room temperature. For purification, the reaction mixture was centrifuged at 7000 rpm for 15 min, and the resulting pellet was resuspended with deionized water. The process was repeated twice to remove unreacted PEG molecules.

Establishment of mouse model

Each mouse was injected intraperitoneally with A20 lymphoma cells (1×106 cells/mL) and mice in the experimental group were injected intravenously with HAuNS-CD138 gold nanoparticles. All mice received NIR laser radiation through the skin surface at 24 h post injection. A group without injection of nanoparticles, a group injected with nanoparticles without NIR laser treatment, and a group injected with nanoparticles without anti-CD138 antibodies were prepared and used as controls.

Detection of Immunoglobulin G2a (IgG2a) by ELISA

Heavy chain-specific, polyclonal rat anti-mouse IgG2a (ABD Serotec, Kidlington, UK) at 5 μg/mL in phosphate buffered saline (PBS) pH 7.2 was coated overnight at 4°C and blocked for 1 h at 37°C using 2% bovine serum albumin. Plates were washed four times with PBS/0.05% Tween 20 between all steps. Serial dilutions of purified mouse IgG2a (R&D System, Minneapolis, USA) were used to generate a standard curve for detection. After addition of primary antibody or standard, the plates were incubated for 1 h at 37°C. Then o-phenylenediamine (Sigma-Aldrich, St. Louis, USA) was added, followed by four washes and blocking for 1 h. After 20 min, the ELISA was terminated by the addition of 50 μl 2M H_2SO_4 and quantified at 490 nm using a Molecular Devices Thermo Max Microplate Plate Reader (USA). Finally, the concentration of IgG2a was determined according to the standard curve.

Results

The amount of IgG2a antibody produced and secreted by A20 tumor cells is an important indicator of A20 lymphoma growth. Therefore, the growth condition of A20 lymphoma in mice can be evaluated by detecting IgG2a concentrations in sera. The mice were first divided into three categories and each category contained seven groups (each group had 10 female BALB/c mice). These three categories were: before NIR; 1 day after NIR treatment; and 4 days after NIR treatment. The seven experimental groups were as follows: Q1, no nanoparticles and no NIR treatment; Q2, targeted nanoparticles and no NIR treatment; Q3, no nanoparticles but NIR treatment; Q4, non-targeted nanoparticles and NIR treatment, sampling after 6 h; Q5, targeted nanoparticles and NIR treatment, sampling after 6 h; Q6, non-targeted nanoparticles and NIR treatment, sampling after 24 h; and Q7, targeted nanoparticles and NIR treatment, sampling after 24 h (Table 1). Subsequent to treatments, A20 cells in the logarithmic phase were washed twice and suspended in PBS, and then injected into BALB/c mice tail vein at 105 cells/mouse. The mice were checked for deaths and abnormal behavior at 24 h post injection. On the basis of previous work, A20 lymphoma would evidently be touched at 6 weeks post injection. At 27 days after inoculation, various nanoparticles were injected into anesthetized mice by the caudal vein. After 72 h, PEG-modified gold nanoparticles in the blood vessels were removed, and at the same time (on the 30th day), mice began to receive radiation therapy.

	Before NIR	1 day after NIR	4 days after NIR
Q1	−nanoparticles	−nanoparticles	−nanoparticles
	−NIR	−NIR	−NIR
Q2	+ targeted nanoparticles	+ targeted nanoparticles	+ targeted nanoparticles
	−NIR	−NIR	−NIR
Q3	+ nanoparticles	+ nanoparticles	+ nanoparticles
	−NIR	−NIR	−NIR
Q4	− targeted nanoparticles	− targeted nanoparticles	− targeted nanoparticles
	+ NIR	+ NIR	+ NIR
	sera collected after 6 hours	sera collected after 6 hours	sera collected after 6 hours
Q5	+ targeted nanoparticles	+ targeted nanoparticles	+ targeted nanoparticles
	+ NIR	+ NIR	+ NIR
	sera collected after 6 hours	sera collected after 6 hours	sera collected after 6 hours
Q6	− targeted nanoparticles	− targeted nanoparticles	− targeted nanoparticles
	+ NIR	+ NIR	+ NIR
	sera collected after 24 hours	sera collected after 24 hours	sera collected after 24 hours
Q7	+ targeted nanoparticles	+ targeted nanoparticles	+ targeted nanoparticles
	+ NIR	+ NIR	+ NIR
	sera collected after 24 hours	sera collected after 24 hours	sera collected after 24 hours

Table 1: Design scheme of experimental groups

Simultaneously, serum levels of IgG2a in each group were determined and the time of determination was set as the 7th, 14th, 21st, 28th, 30th, 31st, and 35th days after inoculation with A20 cells

(set as day 0). The experimental results showed that the basal levels of IgG2a averaged between 0.05 mg/mL and 0.08 mg/mL on day 0. In the first 30 days, all A20 lymphomas of experimental mice without NIR treatment showed a similar growth rate, with no significant difference (Figure 1), although IgG2a levels rose to 0.3 to 0.38 mg/mL. On the first day of NIR treatment, that is, 31 days post inoculation of A20 lymphoma cells, growth delay of the tumor in the Q5 and Q7 experimental groups began to emerge. Compared with the day before, IgG2a levels in the Q5 group was slightly decreased, from 0.31 mg/mL to 0.28 mg/mL, while IgG2a levels in the Q7 group remained at 0.35 mg/ml. Meanwhile, IgG2a levels of the rest of the experimental mice obviously kept increasing. At 4 days after NIR treatment, namely, 35 days after inoculation with A20 cells, lymphomas in Q5 and Q7 showed significant growth delay, and the concentration of IgG2a decreased to 0.24 mg/ml and 0.26 mg/ml, respectively. At the same time, the other groups, including those injected with non-targeted nanoparticles (i.e., HAuNS) and treated by NIR, and those injected with targeted nanoparticles (i.e., HAuNS - CD138) but were not treated by NIR, did not show any delay in tumor growth (Figures 1 and 2). In addition, IgG2a levels reached 0.4–0.5 mg/mL, demonstrating that HAuNS-CD138 nanoparticles have great potential in lymphoma targeted therapy.

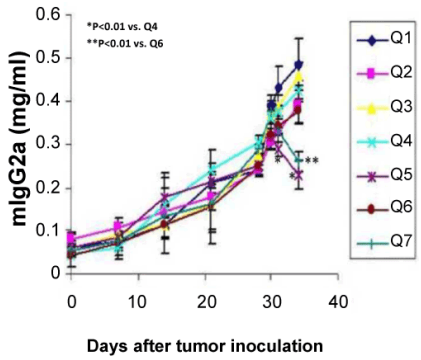

Figure 1: Detection of IgG2a levels in mouse sera by ELISA

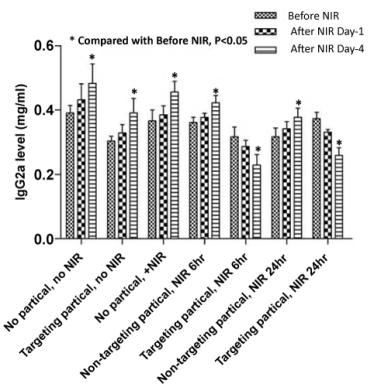

Figure 2: Detection of IgG2a levels after photothermal therapy

In order to investigate the growth of lymphoma further, A20 lymphomas were collected and comparison of their weight showed that it was consistent with IgG2a levels, except that the tumor weight of the Q5 and Q7 groups was significantly decreased (0.25 ± 0.06 g), while the tumor weight of the other experimental groups reached 0.45 ± 0.09 g (Figure 3).

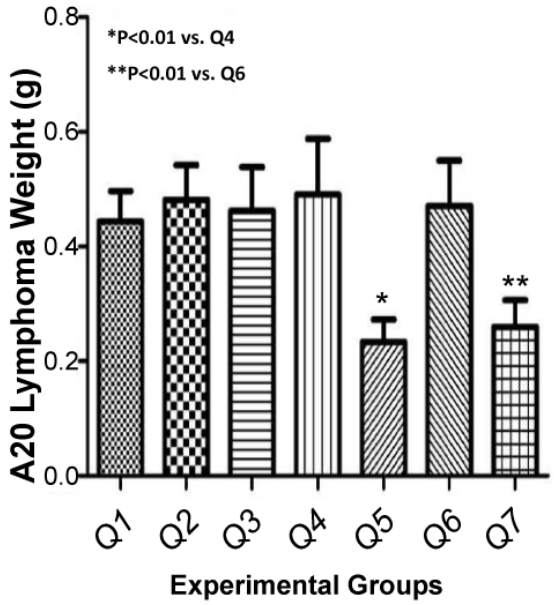

Figure 3: Weight analysis of A20 lymphoma after NIR treatment

Discussion

Cancer is one of the main diseases that affect human health. There are 2.2 million new cases of cancer each year, and deaths caused by cancer are 1.6 million per year, making cancer the top cause of death in China. However, traditional treatments for cancer cannot achieve the goal of tumor eradication because of their side effects and limitations. In recent years, with the rapid development of nanotechnology, it provides a bright prospect for cancer treatment [1,20-25]. In particular, unique optical tunable gold nanomaterials show extensive and important potential in the field of biomedical application. They can be used as a carrier for drugs and biological molecules, as well as an active reagent for biological imaging and photothermal treatment in early diagnosis and treatment [2,26-30].

Most successful applications of nanoparticles for diagnosis and treatment depend on their aggregation at tumor sites [31,32]. The aggregation mainly depends on several molecular mechanisms. Conventionally, nanoparticles can passively aggregate at tumor sites by abnormal leakage of blood vessels around tumors. New angiogenesis is a major feature of tumors and the newly generated blood vessels around the tumor have an irregular shape and lumen diameter (up to 2 μM), which can allow macromolecules and nanoparticles in the blood vessels to be absorbed by the tumor [17,18]. However, nanoparticles without proper coating would be quickly metabolized in blood circulation. Therefore, chemical modification of nanoparticles can effectively improve their retention period in blood circulation.Recent research has shown that PEG-modified nanoparticles have a greatly improved retention period in blood circulation, enhancing their absorption by the tumor. Besides being passively absorbed by cancer cells, nanoparticles are able to recognize proteins or ligands expressed on the surface of tumor cells, facilitating

their active and selective targeting of tumor cells [14-16]. For example, many solid tumors always abnormally overexpress HER2(human epidermalgrowth factor receptor-2), 5α-integrin receptors, or interleukin receptors. Conjugating an antibody to these proteins or ligands to nanoparticles will actively facilitate nanoparticle targeting of these tumor cells. Nanoparticles used for cancer killing can absorb near-infrared light so as to generate heat that will ablate tumor cells under laser radiation. In this study, anti-CD138 antibody was covalently conjugated to gold nanospheres and the conjugates would specifically target A20 lymphoma. With the application of photothermal therapy, gold nanoparticles treated by NIR laser radiation generate heat that is able to destroy tumors [33], achieving the purpose of treatment of the tumor.

In terms of the choice of target molecules, previous experiments showed that A20 lymphoma cells had an high affinity for anti-CD19, anti-CD20, and anti-CD138 antibodies, which reached 92.1%, 88.5%, and 95.2%, respectively (Figure 4). Anti-CD20 monoclonal antibody (rituximab) has been widely used in the treatment of B lymphoma and is currently one of the most successful monoclonal antibody drugs. However, it was found in our study that anti-CD138 antibody had a higher affinity for A20 cells than CD20, so anti-CD138 antibodies were chosen for preparation of antibody-conjugated gold nanospheres. Anti-CD138 antibody recognizes CD138 antigen, which is also called syndecan-1. CD138 is a transmembrane glycoprotein molecule that interacts with extracellular matrix proteins, cell surface molecules, and other soluble proteins [19]. It is also a plasma cell marker that can be used for recognition of B lymphoma and myeloma. The results of this study have confirmed that anti-CD138 antibody is a good targeting molecule for A20 lymphoma, and anti-CD138 antibody-conjugated hollow gold nanoparticles show great potential in clinical therapy.

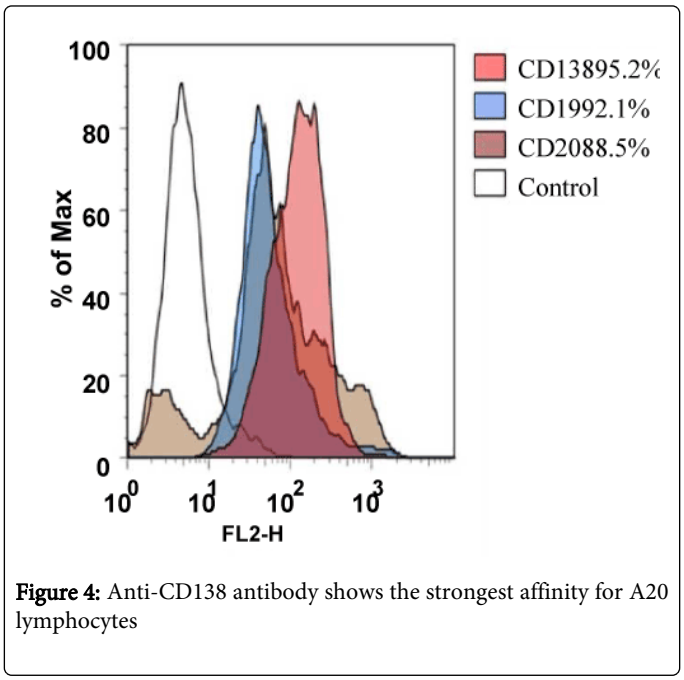

Figure 4: Anti-CD138 antibody shows the strongest affinity for A20 lymphocytes

Our studies raise a number of interesting questions that should be addressed in the future. For instance, it is important to confirm whether the suppression of A20 lymphomas will be sustained over time and whether sustained suppression will require repeated treatment, so long-term studies to evaluate the antitumor activity of targeted HAuNS in combination with near IR-region laser irradiation will need to be carried out to further confirm the short-term results obtained in the current studies. Using a small-molecular-weight(CD138) peptide as atarget and attaching it at the end of PEG chains, we found that receptor-mediated active targeting of lymphoma in vivo. Although our current study has shown promising results inselective photothermal ablation of lymphoma using targeted HAuNS, much work remains to be done to advance thistechnology further into the clinic. For example, more detailedpreclinical studies with regard to clearance, safety, and efficacy of targeted HAuNS need be documented.

Acknowledgements

We thank Dr. Chun Li for helpful discussions and Dr. Wei Lu for assistance with nanoshell preparation. This work was supported by the Priority Academic Program Development of Jiangsu Higher Education Institutions, the National Natural Science Foundation of China (81272476), and Science and Technology Support Program Project of Jiangsu Province (BE2010649, BE2011682).

References

1. Hirsch LR, Stafford RJ, Bankson JA, Sershen SR, Rivera B, et al. (2003) Nanoshell-mediated near-infrared thermal therapy of tumors under magnetic resonance guidance. ProcNatlAcadSci U S A 100: 13549-13554.
2. O'Neal DP, Hirsch LR, Halas NJ, Payne JD, West JL (2004) Photo-thermal tumor ablation in mice using near infrared-absorbing nanoparticles. Cancer Lett 209: 171-176.
3. El-Sayed IH, Huang X, El-Sayed MA (2006) Selective laser photo-thermal therapy of epithelial carcinoma using anti-EGFR antibody conjugated gold nanoparticles. Cancer Lett 239: 129-135.
4. Huang X, Jain PK, El-Sayed IH, El-Sayed MA (2008) Plasmonicphotothermal therapy (PPTT) using gold nanoparticles. Lasers Med Sci 23: 217-228.
5. Li JL, Day D and Gu M (2008) Ultra-low energy threshold for cancer photothermal therapy using transferrin-conjugated gold nanorods. Adv. Mater 20: 3866-3871.
6. Tong L, Zhao Y, Huff TB, Hansen MN, Wei A, et al. (2007) Gold Nanorods Mediate Tumor Cell Death by Compromising Membrane Integrity. Adv Mater 19: 3136-3141.
7. Takahashi H, Niidome T, Nariai A, Niidome Y, Yamada S (2006) Gold nanorodsensitized cell death: microscopic observation of single living cells irradiated by pulsed near-infrared laser light in the presence of gold nanorods. Chem. Letts 35: 500-501.
8. Niidome T, Akiyama Y, Yamagata M, Kawano T, Mori T, et al. (2009) Poly(ethylene glycol)-modified gold nanorods as a photothermalnanodevice for hyperthermia. J BiomaterSciPolym Ed 20: 1203-1215.
9. Ratto F, Matteini P, Rossi F, Menabuoni L, Tiwari N, et al. (2009) Photothermal effects in connective tissues mediated by laser-activated gold nanorods. Nanomedicine 5: 143-151.
10. Niidome T, Akiyama Y, Shimoda K, Kawano T, Mori T, et al. (2008) In vivo monitoring of intravenously injected gold nanorods using near-infrared light. Small 4: 1001-1007.
11. Huff TB, Tong L, Zhao Y, Hansen MN, Cheng JX, et al. (2007) Hyperthermic effects of gold nanorods on tumor cells. Nanomedicine (Lond) 2: 125-132.
12. Schwartzberg AM, Olson TY, Talley CE, Zhang JZ (2006) Synthesis, characterization, and tunable optical properties of hollow gold nanospheres. J PhysChem B 110: 19935-19944.
13. Melancon MP, Lu W, Yang Z, Zhang R, Cheng Z, et al. (2008) In vitro and in vivo targeting of hollow gold nanoshells directed at epidermal growth factor receptor for photothermal ablation therapy. Mol Cancer Ther 7: 1730-1739.

14. Brigger I, Dubernet C, Couvreur P (2002) Nanoparticles in cancer therapy and diagnosis. Adv Drug Deliv Rev 54: 631-651.
15. Arrueboa M, Fernández-Pacheco R, Ibarraa RM, Jesus Santamaria (2007) Magnetic nanoparticles for drug delivery. Nano Today 2: 22-32.
16. Moghimi SM, Hunter AC, Murray JC (2001) Long-circulating and target-specific nanoparticles: theory to practice. Pharmacol Rev 53: 283-318.
17. Hobbs SK, Monsky WL, Yuan F, Roberts WG, Griffith L, et al. (1998) Regulation of transport pathways in tumor vessels: role of tumor type and microenvironment. ProcNatlAcadSci U S A 95: 4607-4612.
18. Kong G, Braun RD, Dewhirst MW (2000) Hyperthermia enables tumor-specific nanoparticle delivery: effect of particle size. Cancer Res 60: 4440-4445.
19. Bayer-Garner IB, Sanderson RD, Dhodapkar MV, Owens RB, Wilson CS (2001) Syndecan-1 (CD138) immunoreactivity in bone marrow biopsies of multiple myeloma: shed syndecan-1 accumulates in fibrotic regions. Mod Pathol 14: 1052-1058.
20. Mintorovitch J, Shamsi K (2000) Eovist Injection and Resovist Injection: two new liver-specific contrast agents for MRI. Oncology (Williston Park) 14: 37-40.
21. Nida DL, Rahman MS, Carlson KD, Richards-Kortum R, Follen M (2005) Fluorescent nanocrystals for use in early cervical cancer detection. GynecolOncol 99: S89-94.
22. Zheng G, Patolsky F, Cui Y, Wang WU, Lieber CM (2005) Multiplexed electrical detection of cancer markers with nanowire sensor arrays. Nat Biotechnol 23: 1294-1301.
23. Cross SE, Jin YS, Rao J, Gimzewski JK (2007) Nanomechanical analysis of cells from cancer patients. Nat Nanotechnol 2: 780-783.
24. Yang J, Lim EK, Lee HJ, Park J, Lee SC, et al. (2008) Fluorescent magnetic nanohybrids as multimodal imaging agents for human epithelial cancer detection. Biomaterials 29: 2548-2555.
25. Stoeva SI, Lee JS, Smith JE, Rosen ST, Mirkin CA (2006) Multiplexed detection of protein cancer markers with biobarcoded nanoparticle probes. J Am ChemSoc 128: 8378-8379.
26. Gobin AM, Lee MH, Halas NJ, James WD, Drezek RA, et al. (2007) Near-infrared resonant nanoshells for combined optical imaging and photothermal cancer therapy. Nano Lett 7: 1929-1934.
27. Ji X, Shao R, Elliott AM, Stafford RJ, Esparza-Coss E, et al. (2007) Bifunctional Gold Nanoshells with a Superparamagnetic Iron Oxide-Silica Core Suitable for Both MR Imaging and Photothermal Therapy. J PhysChem C Nanomater Interfaces 111: 6245.
28. Skrabalak SE, Au L, Lu X, Li X, Xia Y (2007) Gold nanocages for cancer detection and treatment. Nanomedicine (Lond) 2: 657-668.
29. Huang X, El-Sayed IH, QianW, El-Sayed MA (2007) Cancer cells assemble and align gold nanorods conjugated to antibodies to produce highly enhanced, sharp, and polarized surface Raman spectra: a potential cancer diagnostic marker. Nano Lett 7: 1591-1597.
30. Loo C, Lin A, Hirsch L, Lee MH, Barton J, et al. (2004) Nanoshell-enabled photonics-based imaging and therapy of cancer. Technol Cancer Res Treat 3: 33-40.
31. Qian X, Peng XH, Ansari DO, Yin-Goen Q, Chen GZ, et al. (2008) In vivo tumor targeting and spectroscopic detection with surface-enhanced Raman nanoparticle tags. Nat Biotechnol 26: 83-90.
32. Liu Z, Cai W, He L, Nakayama N, Chen K, et al. (2007) In vivo biodistribution and highly efficient tumour targeting of carbon nanotubes in mice. Nat Nanotechnol 2: 47-52.
33. Lu W, Xiong C, Zhang G, Huang Q, Zhang R, et al. (2009) Targeted photothermal ablation of murine melanomas with melanocyte-stimulating hormone analog-conjugated hollow gold nanospheres. Clin Cancer Res 15: 876-886.